FEMS Microbiology Ecology, 97, 2021, fiab110

https://doi.org/10.1093/femsec/fiab110
Advance Access Publication Date: 28 July 2021
Research Article

RESEARCH ARTICLE

Microbial perspective on the giant carbonate ridge Alpha Crucis (Southwestern Atlantic upper slope)

Amanda Gonçalves Bendia[1,*,†], Camila Negrão Signori[1], Fernanda Mancini Nakamura[1], Ana Carolina de Araújo Butarelli[1], Júlia Gasparini Passos[1], Raissa Basti Ramos[1], Luiza Ferreira Soares[1], Michel Michaelovitch de Mahiques[1,2], Paulo Yukio Gomes Sumida[1] and Vivian Helena Pellizari[1]

[1]Instituto Oceanográfico, Universidade de São Paulo, 05508-120, Sao Paulo, Brazil and [2]Instituto de Energia e Ambiente, Universidade de São Paulo, 05508-010, Sao Paulo, Brazil

*Corresponding author: Departamento de Oceanografia Biológica, Instituto Oceanográfico, Universidade de São Paulo. Praça do Oceanográfico, 191. 05508-120 São Paulo, SP, Brazil. Tel: +55 11 30916557; E-mail: amandagb@usp.br

One sentence summary: The first description of the microbiome in the water column and sediments associated with a giant carbonate ridge in the Southwestern Atlantic Ocean.

Editor: Lee Kerkhof

†Amanda Gonçalves Bendia, https://orcid.org/0000-0003-0042-8990

ABSTRACT

Deep-sea carbonate mounds can harbor a wide variety of heterotrophic and chemosynthetic microbial communities, providing biodiversity hotspots among the deep-sea benthic ecosystems. This study examined the bacterial and archaeal diversity and community structure in the water column and sediments associated with a recently described giant carbonate mound named Alpha Crucis Carbonate Ridge (ACCR), located in the Southwestern Atlantic Ocean. Because of the acoustic evidence of gas chimneys from a previous study, we further evaluated the chemosynthetic primary production through *in situ*-simulated dark carbon fixation rates. Pelagic microbial communities varied significantly with depth, showing a high abundance of photosynthetic groups in surface waters and taxa related to nitrification in intermediate and deep waters. The benthic communities from the top of the ACCR were very similar along with the sediment depth, while those from the base of the ACCR showed a clear stratification pattern, with members in the deep strata mainly related to anoxic and chemosynthetic ecosystems. Dark carbon fixation rates were of the same order of magnitude as those of deep-sea cold seeps and hydrothermal vents. Our study provides the first description of the ACCR microbiome and adds new information to help formulate and implement future conservation and management strategies for vulnerable marine ecosystems.

Keywords: chemosynthesis; deep-sea carbonate mound; marine microbiome; microbial community structure; southwestern atlantic ocean

INTRODUCTION

Deep-sea carbonate mounds form semicircular to elongated geomorphologies (carbonate ridges), interpreted as the result of long-term alternation between the growth and demise of cold-water corals (Henriet *et al.* 2014; Lo Iacono, Savini and Basso 2018). Several studies have indicated that their development is controlled by seafloor seepage, ocean currents and water mass

Received: 15 February 2021; **Accepted:** 26 July 2021

structure (Mienis *et al.* 2006; Henriet *et al.* 2014; Lo Iacono, Savini and Basso 2018).

Carbonate can also be precipitated through a biogeochemical process mediated by a consortium of methanotrophic and sulfate-reducing bacteria. In this process, authigenic carbonates are formed as a by-product of the anaerobic oxidation of methane by the microbial consortium coupled with the reduction of sulfate at the sulfate-methane transition zone (Boetius *et al.* 2000; Orcutt *et al.* 2011; Judd *et al.* 2020). The formation of methane-derived authigenic carbonate is related to slow flux seepages and gas venting (Andresen, Huuse and Clausen 2008; Magalhães *et al.* 2012; Boetius and Wenzhöfer 2013). Microorganisms have a major role in carbonate mound stabilization and development by facilitating the diagenetic processes that form the authigenic carbonate layers (Foubert *et al.* 2008; Templer *et al.* 2011).

Previous studies have indicated that deep-sea carbonates and seepages usually support a wide diversity of heterotrophic and chemosynthetic microbial communities, providing biodiversity hotspots in deep-sea benthic ecosystems (e.g. Heijs *et al.* 2006; Marlow *et al.* 2014; Ruff *et al.* 2015, 2019; Jing *et al.* 2020). These microbial communities have been described using different methods, such as 16S rRNA gene sequencing (e.g. Case *et al.* 2015; Ruff *et al.* 2015, 2019) and radioisotopic techniques for measuring chemosynthetic activity (e.g. Steemann-Nielsen 1952; Reinthaler, van Aken and Herndl 2010; Zhou *et al.* 2017; Savvichev *et al.* 2018). In addition, studies suggest some key taxa inhabiting deep-sea carbonates, such as the anaerobic methanotrophic Archaea (ANME)-2 group, methanogenic Archaea (Methanococcales, Methanobacteriales, Methanomicrobiales and Methanosarcinales), Marine Group I and members related to Thermoplasmatales (Aloisi *et al.* 2002; Heijs *et al.* 2006; Ruff *et al.* 2015). Due to the high variability observed among carbonate-associated features worldwide, such as depth, presence or absence of seepage activity, types of substrate and hydrodynamics (Liang *et al.* 2017; Åström *et al.* 2018; Diesing and Thorsnes 2018; Maly *et al.* 2019; Zhou *et al.* 2020), information is still needed on the microbial diversity that inhabits sediments associated with carbonate ridges to improve current knowledge about the carbonate-associated microbiome.

A new carbonate ridge was recently described in the upper slope of the Southwestern (SW) Atlantic Ocean based on interpretation of multibeam bathymetry and high-resolution seismic data from the upper slope of the Santos Basin, Southern Brazilian margin (Maly *et al.* 2019). The Alpha Crucis Carbonate Ridge (ACCR) is the first megastructure of carbonate ridge described along the SW Atlantic margin, comprising an ~17×11-km-wide ring-shaped feature, probably fed by fluids escaping from the subsurface through fractures generated by intense halokinesis (Schattner *et al.* 2018; Maly *et al.* 2019). The acoustic data suggest the presence of gas chimneys and recent to subrecent seepage activity (likely methane); however, this activity has not yet been confirmed by *in-situ* geochemistry analyses and description of chemosynthetic fauna. Furthermore, since this area is associated with other types of gas/fluid escape features, such as pockmarks and depressions, it is a particular example of a hydrocarbon-associated carbonate mound in deep waters (de Mahiques *et al.* 2017; dos Santos *et al.* 2018), which harbors an unknown microbial community likely supported by chemosynthesis. To characterize the ACCR from a microbial perspective, we performed 16S rRNA gene sequencing and calculated *in situ*-simulated rates of dark carbon fixation (DCF) of seawater and sediment samples to determine the bacterial and archaeal structure and diversity, taxonomic composition and chemosynthetic activity. The carbonate mounds of the ACCR are home to vulnerable marine ecosystems (Fink *et al.* 2015; Maly *et al.* 2019) because of their low recovery potential when disturbed. For this reason, the description of microbial diversity associated with these carbonate features is crucial for the development of future conservation strategies.

MATERIALS AND METHODS

Study area and sampling strategy

The study area is located between the 450 and 1250 m isobaths in the central portion of the Santos Basin, southeastern Brazilian margin (Fig. 1A). The area is influenced and shaped by the bottom currents system of Brazil Current (BC) and the Intermediate Western Frontier Current (IWBC) (Fig. 1B) with opposite flow directions. The samples were collected in the ACCR (Fig. 1C). The ACCR was recently described by Maly *et al.* (2019) as a giant ring-shaped carbonate complex surrounding the seabed and flanked by elongated depressions. The oceanographic stations were selected according to the geomorphological pattern observed in the area. Stations P686 and P688 were located on the northwestern portion of the seabed of the complex (named here as the 'base of ACCR'), characterized by the presence of carbonate walls (Maly *et al.* 2019), while stations P685 and P687 were located at the top of the main province of the ACCR (named 'top of ACCR'), dominated by a carbonate ridge comprising the Besnard Mound, which is the highest individual mound of the system (340 m above the seafloor). We observed a high abundance of cold-water corals only in samples from the top of ACCR (Supplementary Fig. 1). A total of 30 sediment samples and 12 water samples were collected in these four stations on board the R/V Alpha Crucis from the Oceanographic Institute of the University of São Paulo in November 2019 (Supplementary Table 1).

We collected the sediment samples using an Ocean Instruments ® box corer (50 cm x 50 cm x 50 cm). Sampling was performed in triplicates per station, except for station P685, at which only one replicate was sampled. At this station, after several attempts, we could only successfully collect one full box-corer due to a large number of deep-sea corals. Therefore, the overlying water was drained before the box corer opening, and four 7 × 20 cm cores were collected for microbial and physical-chemical analyses. The cores were extruded and subsampled in 0–5, 5–10 and 10–15 cm strata and stored in Whirl-pack bags at -80°C. A 5-cm slice for each stratum was defined to get enough sediments for microbiological analyses and represent communities along the different sediment depths. For the DCF analysis, 10 g of sediment of each sample was used for onboard incubations. We also collected one gravity-corer sample at station P686 to analyze microbial communities at a deeper sediment stratum (350 cm).

The water column overlying the ACCR was collected to determine whether water mass characteristics and the pelagic microbial communities differ or not along with the mound. We then collected one water sample per station at three different depths. The first depth comprised the deep water (~530 m), the nearest depth from the bottom of the ACCR. The other depths comprised the intermediate (~280 m) and the surface water (~40 m), which were sampled for comparison with the deep-water samples. Details about sample depths are given in Supplementary Table 1. The water column was sampled using a combined Sea-Bird CTD/Carrousel 911 system with 12 10-L Niskin bottles. Approximately 20 L of each water sample was filtered onboard using a

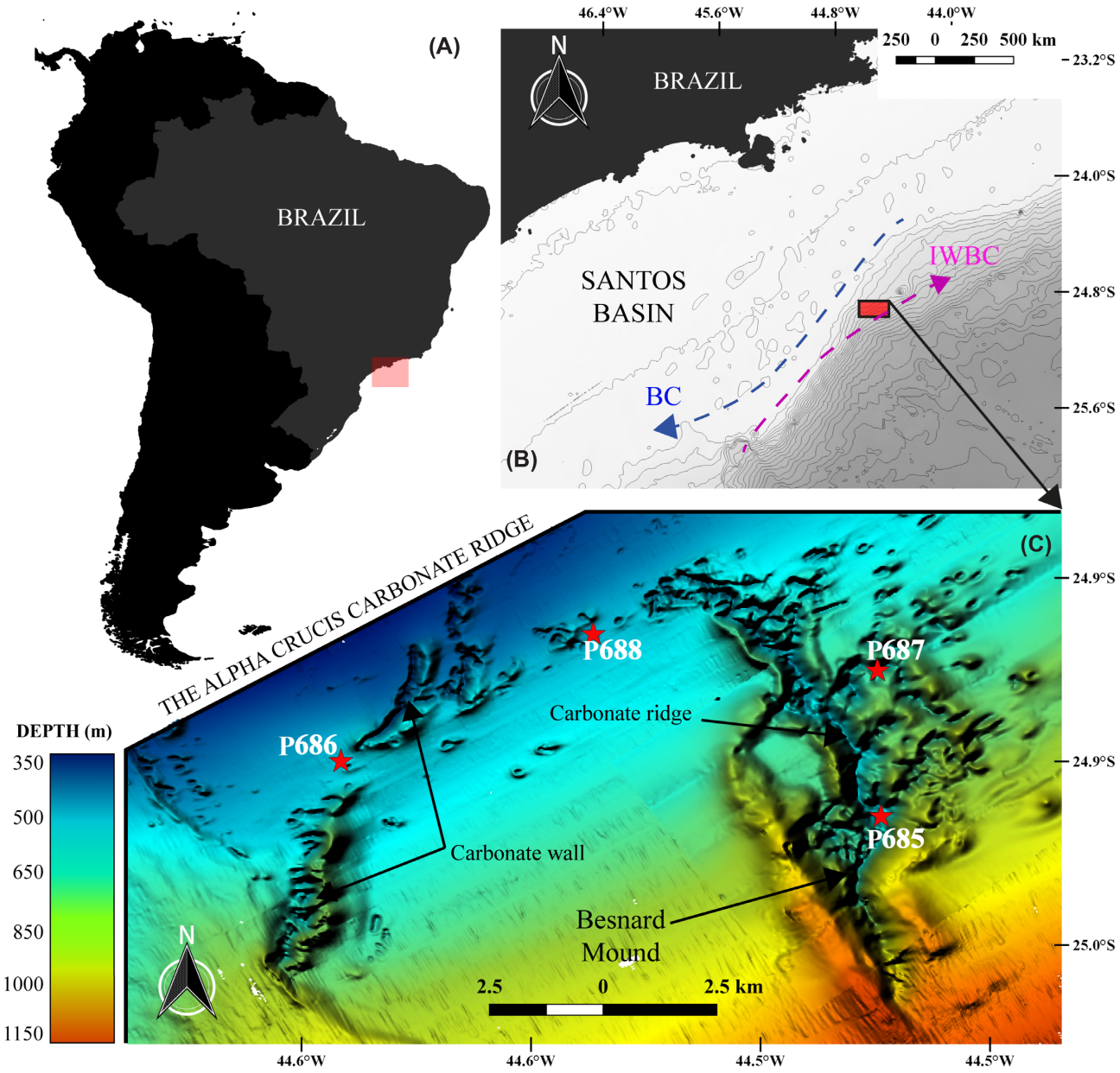

Figure 1. Sampling map showing **(A)** the location of the Alpha Crucis Carbonate Ridge area, **(B)** its geomorphological provinces and **(C)** the sampling sites at the top (P685 and P687) and at the base (P686 and P688) of the mound.

peristaltic pump and 0.22 μm-membrane Sterivex™ filters then frozen at -20åC for molecular analysis. Unfiltered and filtered water samples for chemical analyses were stored in amber flasks at room temperature and in bottles frozen at -20åC. Approximately 2 L of water of each sample was prepared for DCF onboard incubations.

Physical variables and nutrient analysis of water samples

The temperature and salinity of water samples were measured *in situ* using the system CTD-Rosette onboard R/V Alpha Crucis during Cruise 1. Nitrate and nitrite were measured using a SEAL Analytical AutoAnalyzer II and phosphate, silicate and ammonium using a Thermo Scientific Spectrophotometer Evolution 200. Nutrient analyses were performed in the Laboratório de Nutrientes, Micronutrientes e Traços no Mar, at the Oceanographic Institute of the University of São Paulo, São Paulo, Brazil.

DNA extraction and 16 rRNA gene sequencing

DNA extraction of sediment and Sterivex filters was performed using the DNEasy PowerSoil Kit (Qiagen, Hilden, Germany) and DNEasy Powerwater Kit (Qiagen, Hilden, Germany), respectively, following the manufacturing protocols. Extracted DNA was quantified using Qubit dsDNA HS Assay (Thermo-Fisher Scientific, Waltham, MA, USA) and Qubit Fluorometer 1.0 (Thermo-Fisher Scientific). Total extracted DNA from sediment and water samples were sequenced using an Illumina Miseq paired-end system 2 × 350 bp, with the primers 515F-926R (Parada, Needham and Fuhrman 2015), targeting the V3–V4 regions of the 16S rRNA gene. Sequencing was performed by ZymoBIOMICS® Service (Irvine, CA, USA).

Bioinformatics

Raw sequences were imported into QIIME 2 (v.2020.2, https://docs.qiime2.org/) (Bolyen *et al.* 2019) using the q2-tools-import script. DADA2 software was used to obtain a set of observed sequence variants (Callahan, McMurdie and Holmes 2017). Based on the quality scores, the forward reads were truncated at position 270, and the reverse reads at 200, using the q2-dada2-denoise script. Primer sequences were removed using the same script. Taxonomy was assigned through feature-classifier classify-sklearn and SILVA database v138. The phylogenetic tree was built by FastTree (Price, Dehal and Arkin 2009) and the MAFFT aligner (Katoh *et al.* 2002). Alpha and beta diversity metrics were computed through the q2-diversity core-metrics script at a rarefied sampling depth of 32 000 sequences. Statistical differences in alpha diversity indices were calculated by comparing sites and depths (sediment strata or water depth) using the ANOVA test in R (version 3.6.3, package stats v.3.6.2). Beta diversity was measured by weighted Unifrac distance and visualized via non-metric multidimensional scaling (NMDS) using the phyloseq package (Callahan, McMurdie and Holmes 2017) in R (version 3.6.3). Differences in the microbial community structure among sediment strata, water depths and sites were tested by performing a permutational multivariate analysis of variance (PERMANOVA) on the community matrix (Anderson 2001).

Prediction of energetic metabolisms and ecological processes based on the 16S rRNA gene was performed using the FAPROTAX 1.2.3 (Louca, Parfrey and Doebeli 2016). FAPROTAX maps the metabolic and ecological functions using the current literature on cultured strains. We removed from the output FAPROTAX table the categories that are not applied in our study, such as those related to human pathogens. In addition, we decided to maintain both general (e.g. nitrification) and specific FAPROTAX categories (e.g. ammonia oxidation). Although they might represent redundant functions, the general categories often include more than one metabolic pathway. Sequencing data were deposited in the National Center for Biotechnology Information Sequence Read Archives under BioProject ID PRJNA691928.

DCF in water and sediment samples

In situ-simulated incubations in the dark with ^{14}C-bicarbonate (Steemann-Nielsen 1952) with slight modifications (Reinthaler, van Aken and Herndl 2010) were performed to determine the chemosynthetic microbial production of DCF in the water column and sediment strata. First, aliquots of water samples (50 mL) and sediment samples (5 g) were inoculated with 10 μCi ^{14}C-bicarbonate (specific activity 56 mCi mmol^{-1}, Perkin Elmer, USA) and incubated in the dark at an *in situ* temperature for 6–12 h, depending on the sampling area and depth. Incubations were stopped by the addition of formaldehyde (2% final concentration), and the water samples were filtered into 0.22-μm membranes using a vacuum pump and manifold. Next, the membranes and sediment samples were exposed to a fume of concentrated HCl to remove the remaining $^{14}CO_2$. After that, the membranes of the sediments were placed into scintillation vials with 5 mL of scintillation cocktail (Optiphase Hisafe 3, Perkin Elmer) and left in the dark for at least 24 h before being counted (30–60 min per sample, respectively) with a liquid scintillation counter (Perkin Elmer Tricarb 2810 TR). After calculations, the results given in disintegrations per min were converted into production rates of carbon per area and time (μgC m^{-3} h^{-1}) following Steemann-Nielsen (1952) and Teixeira (1973).

To compare the difference within DCF at each depth and each layer, we performed an analysis of variance (ANOVA) followed by Tukey's post hoc multiple-comparison test. Data normality was tested using a Shapiro-Wilk test, and a log(x) transformation was applied when data did not fit normality. The Pearson correlation coefficient was used to examine the relationship between DCF rates and environmental factors. Furthermore, we conducted a simple linear regression analysis on a log scale to evaluate the impact of the water column DCF rates on the sediment rates. A principal component analysis (PCA) was carried out to the correlation matrix to identify the main factors responsible for the total variance on the water column and possible ordination of the samples. Following the PCA, a PERMANOVA based on the Bray-Curtis dissimilarity matrix was performed to statistically determine if any patterns observed in the PCA were valid. The tests mentioned above were carried out using the software PAST v. 4.03 (Hammer, Harper and Ryan 2001).

RESULTS

Physical-chemical parameters of water samples

Seawater temperature ranged from 6.7 to 24.6°C and salinity from 34.4 to 37.2 psu, both decreasing with depth. Phosphate and nitrate presented minimum concentrations (0.05 and 0.33 μmol L^{-1}, respectively) at the surface of station P686 and maximum concentrations (1.58 and 21.37 μmol L^{-1}, respectively) at the deepest stratum of station P686. Silicate concentrations ranged from 0.64 μmol L^{-1} at the surface of station P685 to 50.32 μmol L^{-1} at the most profound depth of station P686. Nitrite concentrations varied from 0.01 μmol L^{-1} at the surface of station P685 to 0.05 μmol L^{-1} at the intermediate depth of station P686. Ammonium ranged from 0.05 μmol L^{-1} at the surface of station P687 to 0.42 μmol L^{-1} at the intermediate depth of station P686. The results of the physical-chemical characteristics are given in Supplementary Table 2.

Alpha diversity of water and sediment samples

We obtained 804 914 sequences distributed among 30 sediment samples and 385 288 sequences among 12 water samples. A mean of 975 amplicon sequence variants (ASVs) (SD ± 270) was detected in sediment samples and 548 ASVs (SD ± 250) in water samples. The values of alpha diversity indices are given in Supplementary Table 3.

Water samples presented a mean number of ASVs of 571 (SD ± 78) for deep waters, 792 (SD ± 66) for intermediate waters and 235 for surface waters (SD ± 72). Shannon mean values were higher in deep (5.08, SD ± 0.28) and intermediate waters (5.76, SD ± 0.12) and lower in surface waters (3.28, SD ± 0.23). All alpha diversity indices (observed ASVs, Chao1, Simpson and Shannon) were significantly higher in deep and intermediate waters than the surface waters.

Sediment samples presented a mean number of ASVs of 934 (SD ± 134) for the 0–5 cm stratum, 954 for 5–10 cm (SD ± 176) and 1004 for 10–15 cm (SD ± 385). The gravity-corer sample (350 cm) exhibited 436 ASVs. The mean values for Shannon were 6.15 (SD ± 0.17) for the 0–5 cm (SD ± 0.32) stratum, 6.11 for 5–10 cm (SD ± 0.32) and 5.86 for 10–15 cm (SD ± 1.24), and 4.52 for the gravity-corer sample (350 cm). No significant difference in alpha diversity indices among sediment strata or location was detected.

Beta diversity of water and sediment samples

We observed a clear and expected separation among water and sediment communities based on NMDS with the weighted Unifrac distance (Fig. 2) and the PERMANOVA analysis. Water communities were shown to be separated by depth ($R^2 = 0.66$, $P = 0.001$) and not by location ($R^2 = 0.07$, $P = 0.991$). Sediment communities were shown to be structured by both strata (depth) ($R^2 = 0.24$, $P = 0.001$) and location ($R^2 = 0.24$, $P = 0.001$).

The pairwise PERMANOVA showed that sediment samples from 0–5 cm were similar at all stations ($P > 0.05$). Samples at 5–15 cm from P685 and P687 (top of ACCR) were very similar to those at 0–5 cm ($P > 0.05$ for all pairwise tests). Samples at 5–15 cm from P686 and P688 (base of ACCR) were significantly distinct from the other samples ($P < 0.05$ for all pairwise tests), suggesting a sediment stratification only at these stations. As expected, the gravity-corer community (P686) was distinct compared with the sediment samples from 0–15 cm.

Microbial community composition in water samples

The most abundant phyla of the surface water samples were Proteobacteria, Actinobacteria, Bacteroidota and Cyanobacteria, containing the classes Alpha- and Gammaproteobacteria, Acidimicrobiia, Bacteroidia and Cyanobacteria, respectively (Fig. 3). Intermediate and deep-water communities included the abundant phyla Proteobacteria, Thermoplasmatota, SAR324 clade (Marine group B), Marinimicrobia (SAR406 clade), Chloroflexi, Bacteroidota, Crenarchaeota and Nitrospinota, and classes such as Dehalococcoidia, Nitrososphaeria, Marinimicrobia (SAR406), Nitrospinia, Marine Group B (SAR324) and Thermoplasmata.

Microbial community composition in sediment samples

The most abundant phyla in sediment samples detected from all depths and stations were Proteobacteria, Planctomycetota, Acidobacteriota, Chloroflexi, NB1-j, Methylomirabilota, Nitrospirota, Bacteroidota and Crenarchaeota (Fig. 4). In addition, samples at 5–10 cm and 10–15 cm from P686 and P688 (base of ACCR) also showed abundant Desulfobacterota, Chloroflexi, Sva0485 and Nanoarchaeota.

Some classes were predominantly found in P686 and P688 (base of ACCR) samples between 5 and 15 cm: Bathyarchaeia, Aminicenantia, Dehalococcoidia, Desulfobacteria, Desulfuromonadia, Nanoarchaeia, Phycisphaerae, Syntrophobacteria, Thermodesulfovibrionia and Thermoplasmata (Supplementary Fig. 2). The Gravity-corer sample (350 cm depth, P688) was mainly composed of the phyla Planctomycetota, Chloroflexi, Thermoplasmatota, Acidobacteria, Hadarchaeota, Asgardarchaeota, Desulfobacterota and Nanoarchaeota, and by the classes Aminicenantia, Dehalococcoidia, Desulfobacteria, Bathyarchaeia, Nanoarchaeia, Phycisphaerae and Thermoplasmata.

Prediction of metabolic and ecological processes

The most abundant predicted functions in surface waters were related to phototrophic processes, comprising relative abundance values of between 21.3 and 24.3% (Fig. 5A). Prediction of heterotrophic processes in surface water samples varied between 0.3 and 1.4%. In intermediate and deep-water samples, nitrification, including ammonia and nitrite oxidation, was the most abundant predicted process within the nitrogen cycle, comprising 1.1 to 18.0% relative abundance among samples. A high proportion of phototrophy was also predicted for intermediate and deep-water samples, varying between 0.07 and 22.2%. Other processes were predicted in minor proportions for intermediate and deep-water samples, such as chemoheterotrophy (1.4–19.4%), dark oxidation of sulfur compounds (0.2–8.9%) and nitrate reduction (0.2–8.3%).

In sediment samples, the most abundant predicted processes (except for the 350-cm core sample) were nitrification, mostly related to ammonia oxidation, comprising percentages of between 16.9 and 45.3% (Fig. 5B). Lower values of nitrification were detected among samples between 10 and 15 cm from the base of ACCR. Chemoheterotrophy was shown to be abundant among all sediments, with values varying between 3.1 and 46.3%. Minor values of chemoheterotrophy were mostly associated with samples from the top of ACCR. Other abundant processes, such as fermentation, were also predicted, mainly in the deepest strata of the base of ACCR, varying between 50 and 3.6%. Less abundant processes, such as nitrate reduction (2.3–0.1%, mostly on top of ACCR), methanogenesis (2.8–0.1%, mainly on the deepest strata of the base of ACCR) and aromatic compound degradation, were predicted to be of a higher proportion (0.6%) for the gravity-corer sample (350 cm). Detailed values of functions predicted by FAPROTAX (relative abundances per sample) and the microbial taxa assigned to the most abundant functions (absolute abundances) are provided in Supplementary Table 4.

Distribution of DCF rates in the water column and sediments

When comparing all stations, station P685 (top of ACCR) and P686 (base of ACCR) presented the highest and lowest DCF rates, respectively, in the pelagic and benthic systems (Fig. 6). In the water column, DCF rates varied from 7.76×10^{-5} μgC m^{-3} h^{-1} at the intermediate depth of station P687 to 1.14×10^{-3} μgC m^{-3} h^{-1} at the intermediate depth of station P685 (Fig. 6B). Even although the DCF rates appear to be higher at deeper depths (Fig. 6A), this difference was not significant ($P > 0.05$).

DCF rates in sediments ranged from 0.18 μgC m^{-3} h^{-1} at the 5–10 cm layer of station P687 to 0.67 μgC m^{-3} h^{-1} at the 10–15 cm layer of station P688 (Fig. 6D). DCF rates in sediments were homogeneous (Fig. 6C) and there was no significant difference ($P > 0.05$) between sediment layers.

Influence of the environmental factors on DCF in water samples

The PCA showed a separation between the surface, intermediate and deep water depths (Fig. 7). The first component (PC1) explained 74.0% of the total variation, being positively correlated with nitrate ($r = 0.99$), depth ($r = 0.99$), phosphate ($r = 0.97$), silicate ($r = 0.96$), DCF ($r = 0.68$), ammonium ($r = 0.54$) and nitrite ($r = 0.47$). The second component (PC2) explained 17.7% of the total variation, being positively correlated with nitrite ($r = 0.82$), ammonium ($r = 0.79$), temperature ($r = 0.29$), salinity ($r = 0.13$) and silicate ($r = 0.04$). The observed separation of samples between depths was significantly different (PERMANOVA, $P = 0.003$).

DCF rates were positively correlated with depth ($r = 0.67$, $P = 0.016$), phosphate ($r = 0.62$, $P = 0.01$) and nitrate ($r = 0.64$, $P = 0.026$), and negatively correlated with temperature ($r = -0.71$, $P = 0.017$) and salinity ($r = -0.66$, $P = 0.016$). The DCF rates in the water column positively correlated with the DCF rates in the sediments ($r = 0.64$, $P = 0.033$) and a simple linear regression showed an explanation of 41% ($R^2 = 0.41$) of the variability of DCF rates in sediment in relation to water.

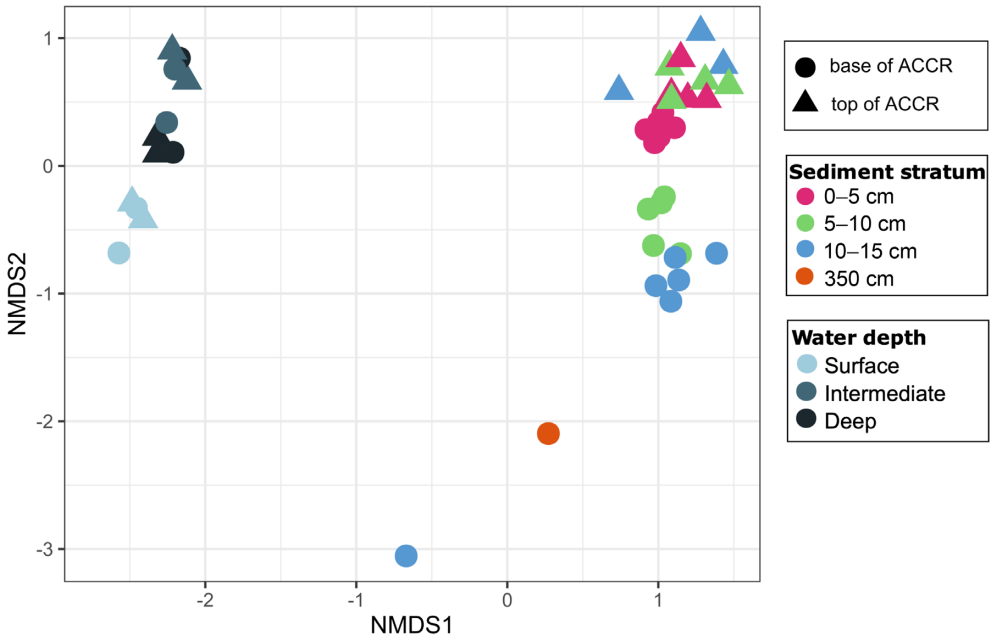

Figure 2. Non-metric multidimensional scaling (NMDS) ordination based on weighted UNIFRAC distances. The circular shapes represent samples from the base of the Alpha Crucis Carbonate Ridge (ACCR), whereas triangles represent those from the top. Colors are classified according to the water depths and sediment strata. Stress value = 0.071.

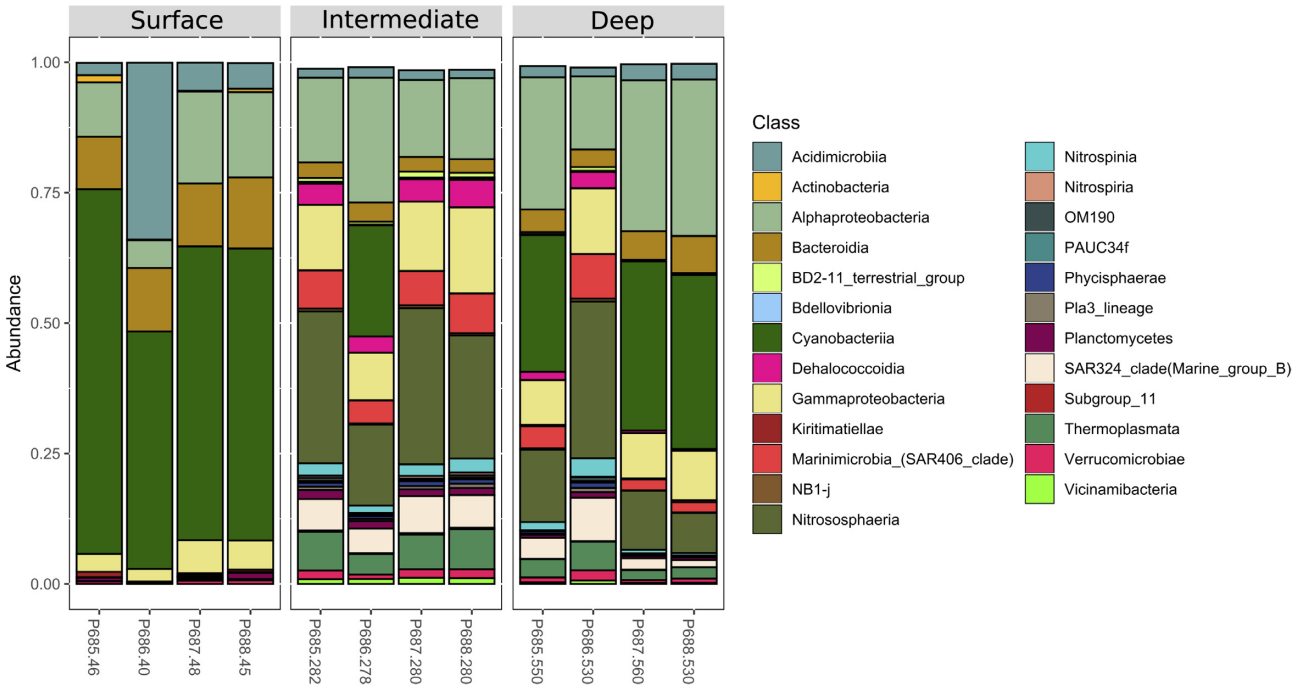

Figure 3. Microbial community composition in water samples associated with the Alpha Crucis Carbonate Ridge. The figure shows the relative abundance of bacterial and archaeal taxonomic groups at class level. Samples are grouped according to the water column depths. Only classes with more than 0.1% of abundance are represented. Sequences were taxonomically classified using the Silva database v. 138.

DISCUSSION

We have provided the first description of the microbial diversity and chemosynthetic activity in the water column and sediment strata associated with a carbonate ridge recently described in the SW Atlantic Ocean. Even although the acoustic data indicates seepages at the foot of the ACCR (Maly *et al.* 2019), no geochemical or biological evidence has been found to confirm the presence of a seep-related ecosystem in the studied area.

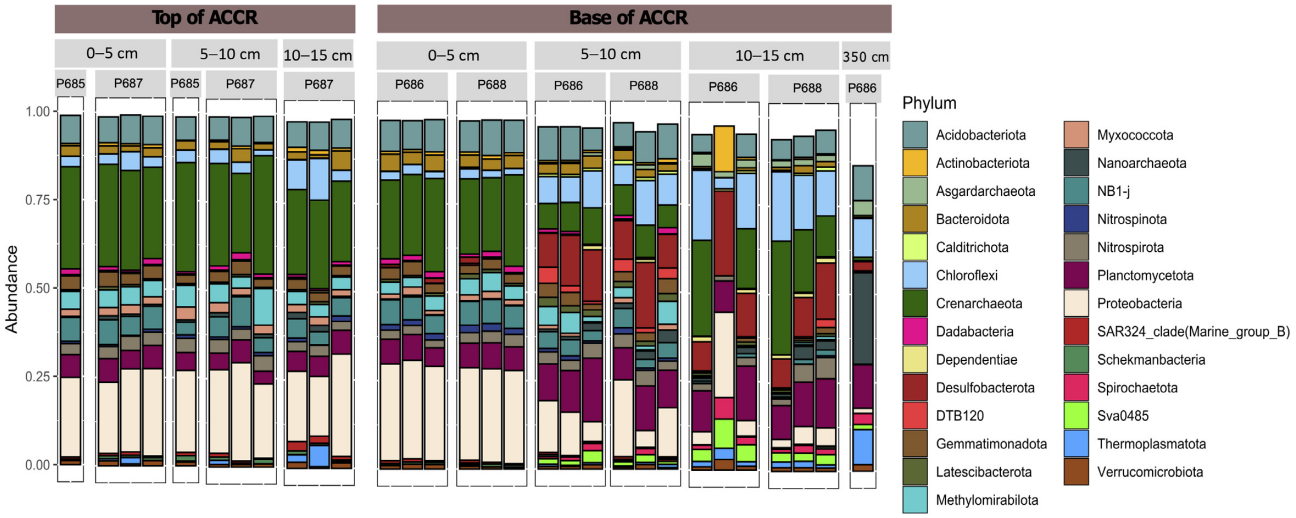

Figure 4. Microbial community composition in sediment samples associated with the Alpha Crucis Carbonate Ridge. The figure shows the relative abundance of bacterial and archaeal taxonomic groups at phylum level. Samples are grouped according to sediment strata and the location on the mound. Only phyla with more than 0.1% of abundance are represented. Sequences were taxonomically classified using the Silva database v. 138.

Microbial diversity in water samples associated with the ACCR

The vertical distribution of physical and chemical parameters of the water column followed typical temperature-salinity diagrams for the SW Atlantic Ocean (Cirano *et al.* 2006), with the presence of the Tropical Water in the surface and the South Atlantic South Water at the bottom. The phosphate, nitrate and silicate concentrations were typical for this region, with low values of the nutrient-depleted waters of the BC (Brandini *et al.* 2000).

We observed significant differences in microbial community structure across water depths, suggesting no influence of the regions of the ACCR on microbial diversity. Surface communities exhibited the lowest alpha diversity indices and an expected high relative abundance of photosynthetic groups, such as Cyanobacteria, and minor proportions of chemoheterotrophs, mainly related to the families Alteromonadaceae, Halomonadaceae and Sphingomonadaceae, according to our predicted metabolic analysis. Intermediate and deep-water communities were more diverse than surface waters, showing a predominance of ammonia-oxidizing Archaea (Nitrososphaeria), the uncultivated bacterioplankton groups Marinimicrobia SAR406 and SAR324 (Marine Group B), the nitrite-oxidizer Nitrospinia, and Thermoplasmata class, mainly represented by Marine Group II. Most of these taxa were already described as abundant in meso- and bathypelagic regions from different locations (e.g. Frank *et al.* 2016; Coutinho *et al.* 2020; Gao *et al.* 2020), except for Marine Group II, which was first described in surface waters as abundant planktonic photoheterotrophs (Rinke *et al.* 2019). However, recent studies have found that some genera within the Marine Group II adapted to nutrient-rich aphotic waters that lost proteorhodopsin genes and then their phototrophic capacity (Rinke *et al.* 2019).

Nitrification was one of the most abundant chemolithotrophic processes predicted for the intermediate and deep-water samples, following the trend of higher nitrate and ammonium concentrations at these depths. The taxa related to nitrification were the nitrite-oxidizer Nitrospinia and the ammonia-oxidizer Nitrososphaeria. Furthermore, several isotopic and molecular studies described ammonia and nitrite oxidation as one of the major biogeochemical processes occurring in the aphotic zone (e.g. Casciotti 2016; Santoro *et al.* 2017; Zhong *et al.* 2020). Regarding the sulfur cycle, the oxidation of sulfur compounds was the overall metabolism predicted for intermediate and deep-water samples and was assigned predominantly within the family Thioglobaceae, which was previously described in deep water masses (Spietz *et al.* 2019; Gifford *et al.* 2020), and within the magnetotactic family Magnetospiraceae, previously found associated with deep-sea polymetallic nodules (Dong *et al.* 2016).

Microbial diversity in sediment samples on the ACCR

Although we did not detect statistical differences in alpha diversity indices among sediment samples, the community structure was significantly different when comparing samples from the top and base areas of the ACCR. However, since the analysis of the R^2 value for depth and location from the PERMANOVA was not necessarily high, we emphasize that other environmental factors (not considered in this study, such as the physical-chemical characteristics of the sediments) might also influence microbial community structure. Sediment communities from the top of ACCR were very similar over a depth of 0 to 15 cm, with no stratification pattern and abundant taxa belonging to classes such as NB1-j, Nitrosphaeria, Methylomirabilia, Gammaproteobacteria and Nitrospiria. Methylomirabilia members were recently described as involved with nitrite-dependent denitrifying anaerobic methane oxidation (Ettwig *et al.* 2010) in different freshwater and marine ecosystems (e.g. Chen, Zhou and Gu 2014; Shen *et al.* 2016; Chen and Gu 2017), and a recent study described for the first time their presence in cold-seep sediments of the South China Sea (Jing *et al.* 2020). The metabolic prediction showed that the nitrogen cycle, mostly nitrification and ammonia oxidation, together with chemoheterotrophy, are probably the most abundant microbial processes occurring in sediments of the top of ACCR. Several of these microbial taxa and their associated ecological processes are ubiquitous in oxic deep-sea benthic ecosystems (e.g. Walsh *et al.* 2016; Hamdan *et al.* 2018; Li *et al.* 2019), including coral carbonate mounds (Templer *et al.* 2011; van Bleijswijk *et al.* 2015).

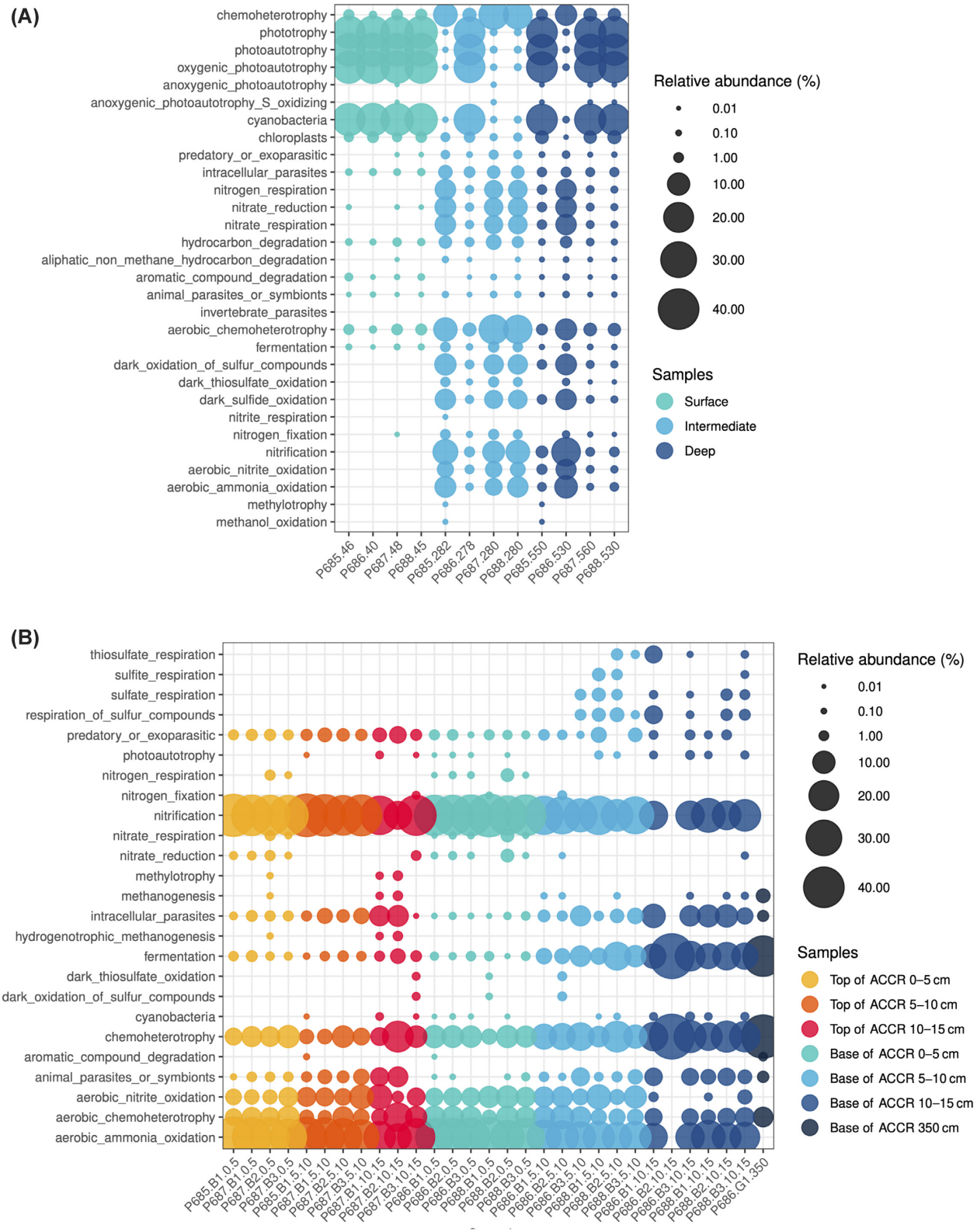

Figure 5. Prediction of metabolic functions and ecological processes on water **(A)** and sediment **(B)** samples of the Alpha Crucis Carbonate Ridge (ACCR) using the FAPROTAX 1.2.3 tool. Values are represented as relative abundances (%) of functions according to each sample. The colors indicate the water depths and the sediment strata. Only functions that showed >0.01% of relative abundance in at least one sample are represented. Categories automatically generated by FAPROTAX that were not related to our study (e.g. human pathogens) were removed. In addition, general and specific FAPROTAX categories were maintained, so that in some cases they might represent redundant taxa and functions (e.g. nitrification and ammonia oxidation).

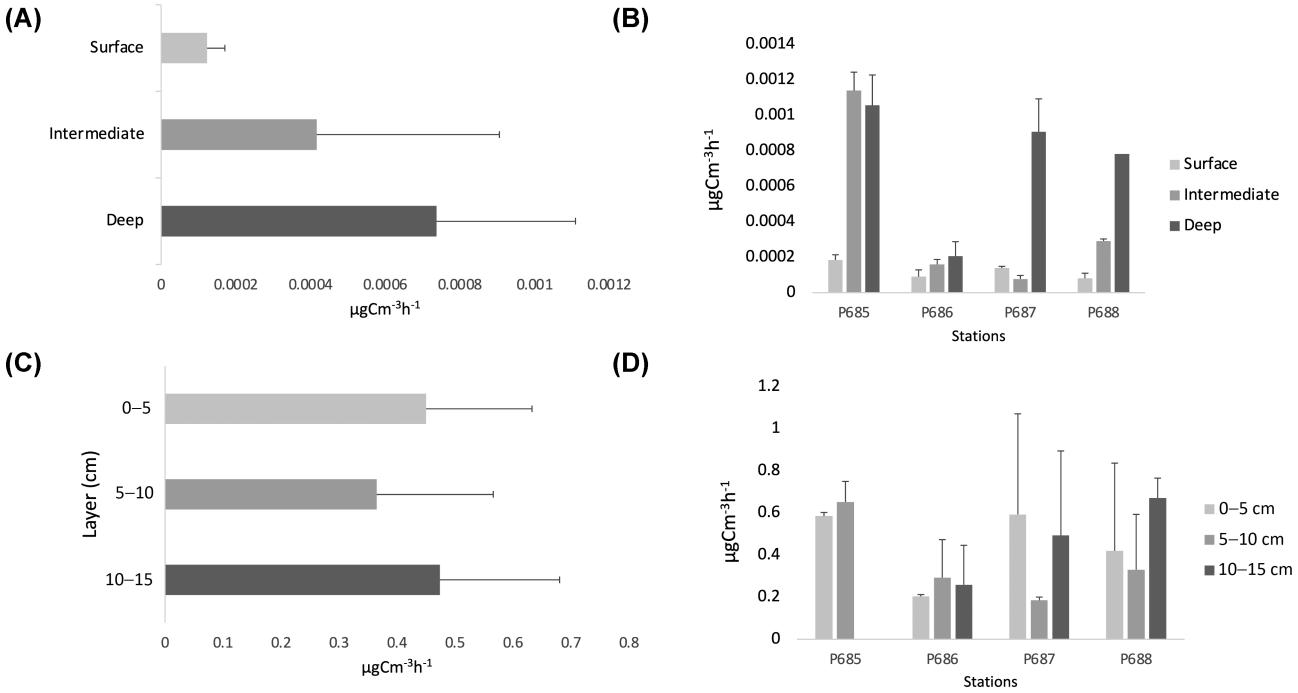

Figure 6. Upper plots: average dark carbon fixation (DCF) rates (µgC.m^{-3}.h^{-1}) of the water column per depth **(A)** and station **(B)**. Lower plots: average DCF rates (µgC.m^{-3}.h^{1}) of the sediment per layer **(C)** and station **(D)**. Data are expressed as mean +/- SD.

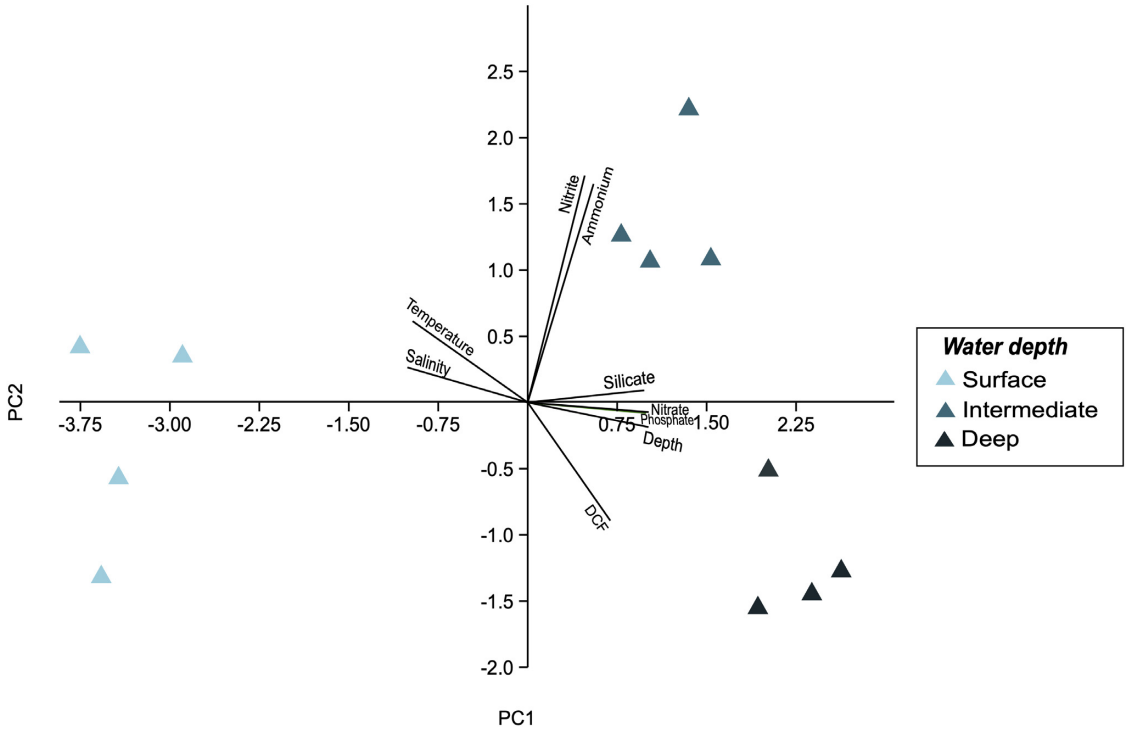

Figure 7. Principal component analysis (PCA) of the water samples on a factor plane and the vectors for dark carbon fixation (DCF), depth, temperature, salinity, phosphate, silicate, nitrate, nitrite and ammonium. Colors are classified according to the water depths. PC1 = 74.0% and PC2 = 17.7%.

The lack of stratification on the top of ACCR likely indicates the influence of the IWBC on the higher ground regions of the ACCR, which strongly flows northeastwards (<0.3 m.s^{-1}), transporting the Antarctic Intermediate Water as a part of the Subtropical Gyre (Viana, Faugères and Stow 1998; Biló *et al.* 2014), and deposits and mixes sediment on the mound (Maly *et al.* 2019). Previous studies performed in other carbonate mounds have indicated that nutrient input by currents likely benefits the coral growth, especially in continental slope regions (Dorschel *et al.* 2007), corroborating what we observed on the ACCR since corals were only observed in samples from the top of the mound. However, little is known about the influence

of the local hydrodynamics and topography of the carbonate mounds on microbial diversity. Van Bleijswijk *et al.* (2015) performed one of the few studies that analyzed this influence on microbial communities from a cold-water coral mound at the Logachev Mound province, Northeastern Atlantic Ocean. They focused primarily on describing differences of microbial communities on overlying water samples (not along sediment depths), and their results indicated a different community between near-bottom water and overlying water (from 5 and 10 m). Since we did not collect near-bottom water samples (~ 0 to 5 m from the ground), nor performed current measurements on the different regions of the mound, more studies are needed to understand the role of local hydrodynamics on benthic and pelagic microbial communities associated with the ACCR.

Communities from the first 5 cm of the base of ACCR were similar to those from the top of the mound, which indicates the influence of the same sediment deposits by the IWBC, but likely in slower rates, as below 5 cm we observed a very distinct community, primarily based on taxa related to anaerobic metabolisms. Community members of 5–15 cm from the base of ACCR have been commonly described in anoxic and chemosynthetic deep-sea benthic ecosystems (e.g. Li *et al.* 2019; Ohkubo *et al.* 2020; Wang *et al.* 2020; Cai *et al.* 2021), which include several uncultivated groups related to the carbon cycle, such as Bathyarchaeia, Aminicenantia, Dehalococcoidia, Nanoarchaeota and Asgardarchaeota, as well as cultivated groups related to the sulfur cycle, such as Desulfobacteria. The main predicted sulfur metabolisms from 5–15 cm of the base of ACCR were sulfate and sulfite respiration performed by the sulfate reducer Desulfobacteria. The subsurface sediment community (350 cm depth) collected on the base of ACCR was mainly composed of uncultivated Bacteria and Archaea, similar to those described for the 5–15 cm samples from the base of ACCR, but with the archaeal members in higher proportions. It is important to highlight that the metabolic predictions performed by FAPROTAX are based on cultured strains (Louca, Parfrey and Doebeli 2016), which has the advantage of the reliability of the assigned functions but does not include uncultivated and new groups related to chemosynthesis with metabolisms still poorly described and not yet confirmed by physiological methods. One example of an uncultivated group that has been suggested as an important contributor to the carbon cycle worldwide is Bathyarchaeia, a class described as global generalist distributed along with anoxic sediments and, according to genomic evidence, has been associated with several metabolic capabilities, such as acetogenesis, methane metabolism, and dissimilatory nitrogen and sulfur reduction (Zhou *et al.* 2017). Other groups, such as Asgardarchaeota, Aminicenantia and Nanoarchaeota, even although widely described in anoxic deep-sea sediments (Farag *et al.* 2014; John *et al.* 2019; Cai *et al.* 2021), still have their metabolic capabilities poorly described, and their role in marine biogeochemical cycles remains unknown.

Previous studies have described the carbonate features in deep-sea ecosystems as habitats of chemolithotrophic and chemoorganotrophic microorganisms that form a unique microbial community structure. However, most studies have been performed with carbonates associated with active cold seeps. By contrast, the microbial diversity from carbonate mounds with distinct geological features and from different ocean basins remains poorly described, such as the ACCR, without confirmation of seepage activity so far. These previous studies, which have collected samples exactly on the regions of the carbonate mounds with seepage activity, showed the presence of a combination of bacterial and archaeal groups, such as ANME, *Methylococcales*, sulfate-reducing Desulfobacterales, sulfide-oxidizing Thiotrichales and Atribacteria (Candidate division JS1) (e.g. Levin 2005; Heijs *et al.* 2006; Marlow *et al.* 2014; Li *et al.* 2019; Ruff *et al.* 2015, 2019; Jing *et al.* 2020). Other taxa such as Methylomirabilota, Flavobacteria, Clostridia, Marine Benthic Group B, Gamma- and Deltaproteobacteria were also described in these studies. The communities described on the ACCR have few members similar to those found in carbonate regions with seepage activity, mainly Methylomirabilota, Desulfobacterota and Thiotrichales (Gammaproteobacteria). However, the ACCR lacks the other key taxa involved with anaerobic methane oxidation, such as those within the ANME group.

Chemosynthetic community and rates on the ACCR

The process of chemosynthesis (herein referred to as DCF) represents a source of newly synthesized organic carbon that is commonly associated with the deep sea but is also observed from surface waters to the sediments (Reinthaler, van Aken and Herndl 2010; Das *et al.* 2011; Bergauer *et al.* 2013; Zhou *et al.* 2017; La Cono *et al.* 2018). In addition, it is commonly associated with redox interfaces that usually occur in cold seeps (Pimenov *et al.* 2000; Savvichev *et al.* 2018) and hydrothermal vents (Tuttle, Wirsen and Jannasch 1983; Wirsen, Jannasch and Molyneaux 1993; Mandernack and Tebo 1999; McNichol *et al.* 2018).

The DCF rates vary significantly in the ocean and, in this study, the observed rates in the water column were similar to those found in the South China Sea (Zhou *et al.* 2017) but were two to six orders of magnitude lower than the rates obtained in the North Atlantic (Reinthaler, van Aken and Herndl 2010; La Cono *et al.* 2018), Tropical Atlantic (Bergauer *et al.* 2013) and Mediterranean Sea (La Cono *et al.* 2018). When compared with those of other deep-sea ecosystems, the obtained DCF rates were two orders of magnitude greater than those of water samples of a shallow cold seep from the Laptev Sea (Savvichev *et al.* 2018) and were similar to the hydrothermal vent fluids of the Crab Spa Vent (McNichol *et al.* 2018). By contrast, the rates were one to five orders of magnitude lower than hydrothermal vents in the Galapagos Rift (Tuttle, Wirsen and Jannasch 1983; Mandernack and Tebo 1999) and six orders of magnitude lower than the Mid-Atlantic Ridge (Wirsen, Jannasch and Molyneaux 1993).

In sediments, the average DCF rates were three orders of magnitude higher than in seawater. When compared with sediments from other deep-sea ecosystems, the DCF rates obtained were up to three orders of magnitude higher than that of a cold seep of the Laptev Sea (Savvichev *et al.* 2018), a pockmark on the Vestnesa Ridge and of the Haakon Mosby Mud Volcano (Pimenov *et al.* 2000).

The observed pattern of relatively higher DCF rates in the sediment than in the water column above was also reported in the Laptev Sea (Savvichev *et al.* 2018). In addition, it is known that the sediments have high availability of reduced sulfur and methane (Whiticar 1990; Orcutt *et al.* 2011), which are energy sources for chemosynthesis and may have led to an intensification of microbial processes in the sediment. Another hypothesis is that in cold seeps, the plume has a significant influence in the benthic zone but a limited role in the water column (Levin *et al.* 2016), which was not the case in our study due to the lack of an active cold seep.

Although both P685 and P687 are located at the top of ACCR, they have very different DCF rates. Relatively higher rates at station P685 may indicate a different environmental condition in the southern ACCR region, hypothetically the influence of the IWBC and the topography of the Besnard Mound (the highest

peak of the ACCR) (see Fig. 1 for location) exposing the southern part of the ACCR to different hydrodynamics. More intense mixing of the water column and sediments can provide greater oxygenation, which is important to chemosynthetic communities, although DCF is, to some extent, possible without dissolved oxygen (Das *et al.* 2011).

In the oceans, DCF is mainly associated with the oxidation of ammonia and nitrite (Reinthaler, van Aken and Herndl 2010; Pachiadaki *et al.* 2017). Although a relatively higher abundance of bacterial and archaeal groups related to these metabolic processes, such as Nitrososphaeria and Nitrospinia, was found, there was no significant correlation between DCF rates and ammonia or nitrite concentrations. This lack of correlation may indicate that part of the DCF in the water column may be attributable to heterotrophs through anaplerotic reactions, which is a relevant process in oligotrophic conditions (González *et al.* 2008; Alonso-Sáez *et al.* 2010) and is mainly determined by the availability of labile organic carbon (Reinthaler, van Aken and Herndl 2010). Thus, active anaplerotic metabolism could explain why DCF in the water column is of the same order of magnitude as in other deep-sea ecosystems. However, further studies are needed to fully comprehend the contribution of the anaplerotic reactions to DCF.

In oxic-anoxic interfaces, chemoautotrophy is expected to be the major contributor to DCF (Zhou *et al.* 2017), as Das *et al.* (2011) show in deep-sea sediments. As mentioned before, the DCF rates obtained in the sediments in this study are comparable with sediments from other cold seeps, which may indicate that chemoautotrophy prevails in sediments of the SW Atlantic Ocean. These high rates may be due to the ACCR-associated seepage, most likely composed of methane (Maly *et al.* 2019), an energy source for chemosynthetic microorganisms (Levin *et al.* 2016). However, as mentioned previously, this type of activity has not yet been confirmed. Furthermore, groups related to sulfate reduction and methane oxidation, such as Desulfobacterota and Methylomirabilota, respectively, were found in sediments, and these microbial processes are typically present in cold-seep sediments (Levin 2005). Therefore, additional studies are recommended to determine which DCF metabolisms prevail in the SW Atlantic carbonate mounds.

CONCLUSIONS

Using a combination of 16S rRNA gene sequencing and *in situ*-simulated rates of DCF, we have characterized the microbial communities and their chemosynthetic activity in the water column and sediments associated with a recently described carbonate mound located in the SW Atlantic Ocean. The microbial communities of the water column are different over depths and not by the location of the ACCR, with taxa related to photoautotrophy more abundant near the surface and those related to nitrification prevalent in intermediate and deep waters. We found that the sediment communities at the top of ACCR were related to oxic sediments and were probably mostly involved with chemoheterotrophy and nitrification processes, besides not presenting stratification at 0–15 cm, probably due to the current influence (IWBC) on the deposition and mixing of sediments in higher regions of the mound. At the base of ACCR, sediment communities at 5–15 cm were composed mainly of taxa found in anoxic deep-sea benthic ecosystems, such as uncultivated and recently described archaeal members assigned within Bathyarchaeia, Nanoarchaeota and Asgardarchaeota. Another important outcome is that the ACCR harbors some taxa previously described in carbonate mounds with seepage activity, such as Desulfobacterota and Methylomirabilota, but lacks the key taxa involved with anaerobic methane oxidation, as those within the ANME group. DCF rates were relevant for the area, comparable with deep-sea cold seeps and hydrothermal vents. However, it is still unclear which metabolic pathways are the main contributors to the DCF, and further studies are underway to reveal the active chemosynthetic members in the ACCR. Finally, our study contributes to describing the deep-sea carbonate microbiome and adds new information for future management and conservation strategies of these geological features, considering vulnerable marine ecosystems that urge a better understanding.

SUPPLEMENTARY DATA

Supplementary data are available at *FEMSEC* online.

FUNDING

BIOIL Project (Shell Brasil) supported the following fellowships: AGB and FMN postdoctoral fellowships; RBR Ph.D. fellowship; ACAB Master's fellowship and LSF Scientific Initiation fellowship. JGP was supported by Master's fellowships from the Federal Agency for the Support and Evaluation of Graduate Education—CAPES.

AUTHOR CONTRIBUTIONS

PYGS conceived and designed the research; CNS, MMdeM, PYGS and VHP coordinated the research, contributed reagents, materials, analysis tools and data; all authors conceived and designed the sampling; AGB, FMN, LFS, MMdeM, PYGS, RBR and VHP collected the samples; all authors conceived and designed the experiments; all authors analyzed and interpreted the data; AGB, CNS, FMN and JGP wrote the manuscript. All authors contributed to the final version of the manuscript.

ACKNOWLEDGEMENTS

This research was carried out in association with the ongoing R&D project registered as ANP 21012–0, 'MARINE LIFE—BMC—OIL AND GAS SEEPS (BIOIL)' (Universidade de São Paulo / Shell Brasil / ANP)—'Avaliação da Biologia e Geoquímica de Exsudações de Óleo e Gás na Costa Sudeste do Brasil', sponsored by Shell Brasil under the ANP R&D levy as 'Compromisso de Investimentos com Pesquisa e Desenvolvimento'. MMdeM acknowledges the Brazilian National Council of Scientific and Technological Development (CNPq, grant 300962/2018–5). We are very thankful to the research teams of LECOM and MicrOcean Lab and Rosa C. Gamba for their sampling and scientific support. We thank the captain and the crew of the R/V Alpha Crucis (IO-USP, FAPESP Process number 2010/06147–5) for the essential support during the I BIOIL oceanographic cruise.

Conflict of interest . The authors declare that the research was conducted in the absence of any commercial or financial relationships that could be construed as a potential conflict of interest.

REFERENCES

Aloisi G, Bouloubassi I, Heijs SK *et al.* CH4-consuming microorganisms and the formation of carbonate crusts at cold seeps. *Earth Planet Sci Lett* 2002;**203**:195–203.

Alonso-Sáez L, Galand PE, Casamayor EO *et al.* High bicarbonate assimilation in the dark by Arctic bacteria. *ISME J* 2010;**4**:1581–90.

Anderson MJ. Permutation tests for univariate or multivariate analysis of variance and regression. *Can J Fish Aquat Sci* 2001. https://doi.org/10.1139/f01-004.

Andresen KJ, Huuse M, Clausen OR. Morphology and distribution of Oligocene and Miocene pockmarks in the Danish North Sea – implications for bottom current activity and fluid migration. *Basin Res* 2008;**20**:445–66.

Åström EKL, Carroll ML, Ambrose WG *et al.* Methane cold seeps as biological oases in the high-Arctic deep sea. *Limnol Oceanogr* 2018;**63**:S209–31.

Bergauer K, Sintes E, van Bleijswijk J *et al.* Abundance and distribution of archaeal acetyl-CoA/propionyl-CoA carboxylase genes indicative for putatively chemoautotrophic Archaea in the tropical Atlantic's interior. *FEMS Microbiol Ecol* 2013;**84**:461–73.

Biló TC, da Silveira ICA, Belo WC *et al.* Methods for estimating the velocities of the Brazil Current in the pre-salt reservoir area off southeast Brazil (23○ S–26○ S). *Ocean Dyn* 2014;**64**: 1431–46.

Boetius A, Ravenschlag K, Schubert CJ *et al.* A marine microbial consortium apparently mediating anaerobic oxidation of methane. *Nature* 2000;**407**:623–6.

Boetius A, Wenzhöfer F. Seafloor oxygen consumption fuelled by methane from cold seeps. *Nat Geosci* 2013;**6**:725–34.

Bolyen E, Rideout JR, Dillon MR *et al.* Reproducible, interactive, scalable and extensible microbiome data science using QIIME 2. *Nat Biotechnol* 2019;**37**:852–7.

Brandini FP, Boltovskoy D, Piola A *et al.* Multiannual trends in fronts and distribution of nutrients and chlorophyll in the southwestern Atlantic (30–62°S). *Deep Sea Res Part I* 2000;**47**:1015–33.

Cai M, Richter-Heitmann T, Yin X *et al.* Ecological features and global distribution of Asgard Archaea. *Sci Total Environ* 2021;**758**:143581.

Callahan BJ, McMurdie PJ, Holmes SP. Exact sequence variants should replace operational taxonomic units in marker-gene data analysis. *ISME J* 2017;**11**:2639–43.

Casciotti KL. Nitrogen and oxygen isotopic studies of the marine nitrogen cycle. *Annu Rev Mar Sci* 2016;**8**:379–407.

Case DH, Pasulka AL, Marlow JJ *et al.* Methane seep carbonates host distinct, diverse, and dynamic microbial assemblages. *mBio* 2015;**6**:e01348–15.

Chen J, Gu J-D. Faunal burrows alter the diversity, abundance, and structure of AOA, AOB, anammox and n-damo communities in coastal mangrove sediments. *Microb Ecol* 2017;**74**:140–56.

Chen J, Zhou Z-C, Gu J-D. Occurrence and diversity of nitrite-dependent anaerobic methane oxidation bacteria in the sediments of the South China Sea revealed by amplification of both 16S rRNA and pmoA genes. *Appl Microbiol Biotechnol* 2014;**98**:5685–96.

Cirano M, Mata MM, Campos EJD *et al.* A circulação oceânica de larga-escala na região oeste do Atlântico Sul com base no modelo de circulação Global OCCAM. *Rev Bras Geofísica* 2006;**24**:209–30.

Coutinho FH, von Meijenfeldt FAB, Walter JM *et al.* Ecogenomics and metabolic potential of the South Atlantic Ocean microbiome. *Sci Total Environ* 2020;**765**:142758.

Das A, Sujith PP, Shashikant Mourya B *et al.* Chemosynthetic activity prevails in deep-sea sediments of the Central Indian Basin. *Extremophiles* 2011;**15**:177–89.

de Mahiques MM, Schattner U, Lazar M *et al.* An extensive pockmark field on the upper Atlantic margin of Southeast Brazil: spatial analysis and its relationship with salt diapirism. *Heliyon* 2017;**3**:e00257.

Diesing M, Thorsnes T. Mapping of cold-water coral carbonate mounds based on geomorphometric features: an object-based approach. *Geosciences* 2018;**8**:34.

Dong Y, Li J, Zhang W *et al.* The detection of magnetotactic bacteria in deep sea sediments from the east Pacific Manganese Nodule Province. *Environ Microbiol Rep* 2016;**8**:239–49.

Dorschel B, Hebbeln D, Foubert A *et al.* Hydrodynamics and cold-water coral facies distribution related to recent sedimentary processes at Galway Mound west of Ireland. *Mar Geol* 2007;**244**:184–95.

dos Santos RF, Nagaoka D, Ramos RB *et al.* Metal/Ca ratios in pockmarks and adjacent sediments on the SW Atlantic slope: implications for redox potential and modern seepage. *J Geochem Explor* 2018;**192**:163–73.

Ettwig KF, Butler MK, Le Paslier D *et al.* Nitrite-driven anaerobic methane oxidation by oxygenic bacteria. *Nature* 2010;**464**:543–8.

Farag IF, Davis JP, Youssef NH *et al.* Global patterns of abundance, diversity and community structure of the Aminicenantes (candidate phylum OP8). *PLoS One* 2014;**9**:e92139.

Fink HG, Wienberg C, De Pol-Holz R *et al.* Spatio-temporal distribution patterns of Mediterranean cold-water corals (Lophelia pertusa and Madrepora oculata) during the past 14,000 years. *Deep Sea Res Part I* 2015;**103**:37–48.

Foubert A, Depreiter D, Beck T *et al.* Carbonate mounds in a mud volcano province off north-west Morocco: key to processes and controls. *Mar Geol* 2008;**248**:74–96.

Frank AH, Garcia JAL, Herndl GJ *et al.* Connectivity between surface and deep waters determines prokaryotic diversity in the North Atlantic Deep Water. *Environ Microbiol* 2016;**18**:2052–63.

Gao P, Qu L, Du G *et al.* Bacterial and archaeal communities in deep sea waters near the Ninetyeast Ridge in Indian Ocean. *J Oceanol Limnol* 2020;**39**:582–97.

Gifford SM, Zhao L, Stemple B *et al.* Microbial niche diversification in the Galápagos Archipelago and its response to El Niño. *Front Microbiol* 2020;**11**:5194.

González JM, Fernández-Gómez B, Fernàndez-Guerra A *et al.* Genome analysis of the proteorhodopsin-containing marine bacterium Polaribacter sp. MED152 (Flavobacteria). *Proc Natl Acad Sci* 2008;**105**:8724–9.

Hamdan LJ, Salerno JL, Reed A *et al.* The impact of the Deepwater Horizon blowout on historic shipwreck-associated sediment microbiomes in the northern Gulf of Mexico. *Sci Rep* 2018;**8**:9057.

Hammer O, Harper DAT, Ryan PD. PAST: paleontological statistics software package for education and data analysis. *Palaeontol Electron* 2001;**9**:1–9.

Heijs SK, Aloisi G, Bouloubassi I *et al.* Microbial community structure in three deep-sea carbonate crusts. *Microb Ecol* 2006;**52**:451–62.

Henriet JP, Hamoumi N, Da Silva AC *et al.* Carbonate mounds: from paradox to World Heritage. *Mar Geol*. 2014;**352**:89–110.

Jing H, Wang R, Jiang Q *et al.* Anaerobic methane oxidation coupled to denitrification is an important potential methane sink in deep-sea cold seeps. *Sci Total Environ* 2020;**748**:142459.

John ES, Flores GE, Meneghin J *et al.* Deep-sea hydrothermal vent metagenome-assembled genomes provide insight into the phylum Nanoarchaeota. *Environ Microbiol Rep* 2019;**11**:262–70.

Judd A, Noble-James T, Golding N *et al.* The Croker Carbonate Slabs: extensive methane-derived authigenic carbonate in

the Irish Sea—nature, origin, longevity and environmental significance. *Geo-Mar Lett* 2020;**40**:423–38.

Katoh K, Misawa K, Kuma K *et al.* MAFFT: a novel method for rapid multiple sequence alignment based on fast Fourier transform. *Nucleic Acids Res* 2002;**30**:3059–66.

La Cono V, Ruggeri G, Azzaro M *et al.* Contribution of bicarbonate assimilation to carbon pool dynamics in the deep Mediterranean Sea and cultivation of actively nitrifying and CO_2-fixing Bathypelagic prokaryotic consortia. *Front Microbiol* 2018;**9**:e00003.

Levin L. *Ecology of Cold Seep Sediments: Interactions of Fauna with Flow, Chemistry and Microbes, Oceanography and Marine Biology*. CRC Press, 2005. https://doi.org/10.1201/9781420037449-3.

Levin LA, Baco AR, Bowden DA *et al.* Hydrothermal vents and methane seeps: rethinking the sphere of influence. *Front Mar Sci* 2016;**3**:e00072.

Li Y, Cao W, Wang Y *et al.* Microbial diversity in the sediments of the southern Mariana Trench. *J Oceanol Limnol* 2019;**37**:1024–9.

Liang Q, Hu Y, Feng D *et al.* Authigenic carbonates from newly discovered active cold seeps on the northwestern slope of the South China Sea: constraints on fluid sources, formation environments, and seepage dynamics. *Deep Sea Res Part I* 2017;**124**:31–41.

Lo Iacono C, Savini A, Basso D. Cold-Water Carbonate Bioconstructions. In: Micallef A, Krastel S, Savini A (eds). *Submarine Geomorphology*. Cham: Springer Geology. Springer International Publishing, 2018, 425–55. https://doi.org/10.1007/978-3-319-57852-1_22.

Louca S, Parfrey LW, Doebeli M. Decoupling function and taxonomy in the global ocean microbiome. *Science* 2016;**353**:1272–7.

Magalhães VH, Pinheiro LM, Ivanov MK *et al.* Formation processes of methane-derived authigenic carbonates from the Gulf of Cadiz. *Sediment Geol* 2012;**243-244**:155–68.

Maly M, Schattner U, Lobo FJ *et al.* The Alpha Crucis Carbonate Ridge (ACCR): discovery of a giant ring-shaped carbonate complex on the SW Atlantic margin. *Sci Rep* 2019;**9**:18697.

Mandernack KW, Tebo BM. In situ sulfide removal and CO_2 fixation rates at deep-sea hydrothermal vents and the oxic/anoxic interface in Framvaren Fjord, Norway. *Mar Chem* 1999;**66**:201–13.

Marlow JJ, Steele JA, Case DH *et al.* Microbial abundance and diversity patterns associated with sediments and carbonates from the methane seep environments of Hydrate Ridge, OR. *Front Mar Sci* 2014;**1**:e00044.

McNichol J, Stryhanyuk H, Sylva SP *et al.* Primary productivity below the seafloor at deep-sea hot springs. *Proc Natl Acad Sci* 2018;**115**:6756–61.

Mienis F, van Weering T, de Haas H *et al.* Carbonate mound development at the SW Rockall Trough margin based on high resolution TOBI and seismic recording. *Mar Geol* 2006;**233**:1–19.

Ohkubo S, Saito T, Azad MAK *et al.* Microbial community structures in terrestrial subsurface sediments from the southern Kanto Plain, Japan. *Geomicrobiol J* 2020;**37**:595–602.

Orcutt BN, Sylvan JB, Knab NJ *et al.* Microbial ecology of the dark ocean above, at, and below the seafloor. *Microbiol Mol Biol Rev* 2011;**75**:361–422.

Pachiadaki MG, Sintes E, Bergauer K *et al.* Major role of nitrite-oxidizing bacteria in dark ocean carbon fixation. *Science* 2017;**358**:1046–51.

Parada AE, Needham DM, Fuhrman JA. Every base matters: assessing small subunit rRNA primers for marine microbiomes with mock communities, time series and global field samples.*Environ Microbiol* 2015. DOI: 10.1111/1462-2920.13023.

Pimenov NV, Savvichev AS, Rusanov II *et al.* Microbiological processes of the carbon and sulfur cycles at cold methane seeps of the North Atlantic. *Microbiology* 2000;**69**:709–20.

Price MN, Dehal PS, Arkin AP. Fasttree: computing large minimum evolution trees with profiles instead of a distance matrix. *Mol Biol Evol* 2009;**26**:1641–50.

Reinthaler T, van Aken HM, Herndl GJ. Major contribution of autotrophy to microbial carbon cycling in the deep North Atlantic's interior. *Deep Sea Res Part II* 2010;**57**:1572–80.

Rinke C, Rubino F, Messer LF *et al.* A phylogenomic and ecological analysis of the globally abundant Marine Group II Archaea (Ca. Poseidoniales ord. nov.). *ISME J* 2019;**13**:663–75.

Ruff SE, Biddle JF, Teske AP *et al.* Global dispersion and local diversification of the methane seep microbiome. *Proc Natl Acad Sci* 2015;**112**:4015–20.

Ruff SE, Felden J, Gruber-Vodicka HR *et al.* In situ development of a methanotrophic microbiome in deep-sea sediments. *ISME J* 2019;**13**:197–213.

Santoro AE, Saito MA, Goepfert TJ *et al.* Thaumarchaeal ecotype distributions across the equatorial Pacific Ocean and their potential roles in nitrification and sinking flux attenuation. *Limnol Oceanogr* 2017;**62**:1984–2003.

Savvichev AS, Kadnikov VV, Kravchishina MD *et al.* Methane as an organic matter source and the trophic basis of a laptev sea cold seep microbial community. *Geomicrobiol J* 2018;**35**:411–23.

Schattner U, Lobo FJ, García M *et al.* A detailed look at diapir piercement onto the ocean floor: new evidence from Santos Basin, offshore Brazil. *Mar Geol* 2018;**406**:98–108.

Shen L-D, Hu B-L, Liu S *et al.* Anaerobic methane oxidation coupled to nitrite reduction can be a potential methane sink in coastal environments. *Appl Microbiol Biotechnol* 2016;**100**:7171–80.

Spietz RL, Lundeen RA, Zhao X *et al.* Heterotrophic carbon metabolism and energy acquisition in Candidatus Thioglobus singularis strain PS1, a member of the SUP05 clade of marine Gammaproteobacteria. *Environ Microbiol* 2019;**21**:2391–401.

Steemann-Nielsen E. The use of radio-active carbon (C14) for measuring organic production in the sea. *ICES J Mar Sci* 1952;**18**:117–40.

Teixeira C. Introdução aos métodos para medir a produção primária do fitoplâncton marinho. *Bol Inst Ocean* 1973;**22**:59–92.

Templer SP, Wehrmann LM, Zhang Y *et al.* Microbial community composition and biogeochemical processes in cold-water coral carbonate mounds in the Gulf of Cadiz, on the Moroccan margin. *Mar Geol* 2011;**282**:138–48.

Tuttle JH, Wirsen CO, Jannasch HW. Microbial activities in the emitted hydrothermal waters of the Galápagos rift vents. *Mar Biol* 1983;**73**:293–9.

van Bleijswijk JDL, Whalen C, Duineveld GCA *et al.* Microbial assemblages on a cold-water coral mound at the SE Rockall Bank (NE Atlantic): interactions with hydrography and topography. *Biogeosciences* 2015;**12**:4483–96.

Viana AR, Faugères J-C, Stow DAV. Bottom-current-controlled sand deposits — a review of modern shallow- to deep-water environments. *Sediment Geol* 1998;**115**:53–80.

Walsh EA, Kirkpatrick JB, Rutherford SD *et al.* Bacterial diversity and community composition from seasurface to subseafloor. *ISME J* 2016;**10**:979–89.

Wang L, Liu R, Wei X *et al.* Transitions in microbial communities along two sediment cores collected from the landward walls of the New Britain trench. *Mar Biol* 2020;**167**:172.

Whiticar MJ. A geochemial perspective of natural gas and atmospheric methane. *Org Geochem, Proceedings of the 14th International Meeting on Organic Geochemistry* 1990;**16**:531–47.

Wirsen CO, Jannasch HW, Molyneaux SJ. Chemosynthetic microbial activity at Mid-Atlantic Ridge hydrothermal vent sites. *J Geophys Res* 1993;**98**:9693–703.

Zhong H, Lehtovirta-Morley L, Liu J *et al.* Novel insights into the Thaumarchaeota in the deepest oceans: their metabolism and potential adaptation mechanisms. *Microbiome* 2020; **8**:78.

Zhou J, Du M, Li J *et al.* Phosphorus species in deep-sea carbonate deposits: implications for phosphorus cycling in cold seep environments. *Minerals* 2020;**10**:645.

Zhou W, Liao J, Guo Y *et al.* High dark carbon fixation in the tropical South China Sea. *Cont Shelf Res* 2017;**146**:82–8.